Zeitschrift: IABSE congress report = Rapport du congrès AIPC = IVBH Kongressbericht

Band: 12 (1984)

Rubrik: VIII. Snow and ice effects on structures

Download PDF: 23.01.2026

ETH-Bibliothek Zürich, E-Periodica, https://www.e-periodica.ch

SEMINAR

VIII

Snow and Ice Effects on Structures

Effets de la neige et de la glace sur les structures

Wirkung von Schnee und Eis auf Tragwerke

Chairman: K. Widbom, Finland

Coordinator: R.A. Dorton, Canada

General Reporter: R. Booth, Canada

The theme has been introduced by the General Reporter in the Introductory Report of the 12th Congress, available at the IABSE Secretariat.

Leere Seite

Blank page

Page vide

Damages Due to Snow Loads
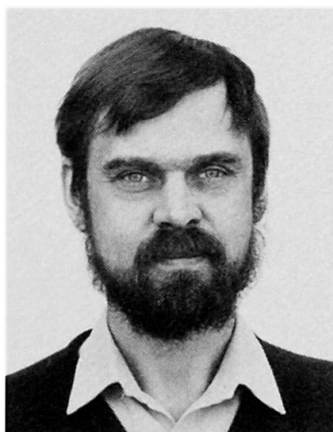
Dommages causés par des charges de neige

Durch Schneelast verursachte Bauschäden

Germund JOHANSSON
Tekn. lic., Lecturer
Chalmers Univ. Technol.
Göteborg, Sweden

Germund Johansson, born 1937, obtained his civil engineering degree at Chalmers Univ. of Technology in 1962. After some years at a consulting firm for geotechnical problems he joined the Dep. of Steel and Timber Structures at Chalmers Univ. of Technology. His research interests include steel structures, roofs, and structural damage due to snow, wind etc.

Bengt JOHANNESSON
Civ. Eng., Ph.D.
Chalmers Univ. Technol.
Göteborg, Sweden

Bengt Johannesson, born 1944, obtained his civil engineering degree at Chalmers Univ. of Technology, in 1972. For two years he worked as a designer in a glulam factory. After returning to CTH, Dept. of Steel and Timber Structures, he spent most of the time in research on structural timber. For some years he has also been working for the National Testing Institute in Sweden. He received his Ph.D. in 1983.

SUMMARY
Structural failures caused by snow loads are discussed. Nearly one hundred failures have been investigated and some examples are given. Nearly all of the structures involved were light-weight steel or timber structures. The failures are mostly due to mistakes in the design or manufacture.

RESUME
Cet article présente une étude de dommages causés à des structures par des charges de neige. Près de cent cas ont été examinés, et pratiquement tous concernent des structures légères en acier ou en bois. Ils sont apparus surtout à la suite d'erreurs dans la conception ou la fabrication. Quelques exemples ont été sélectionnés.
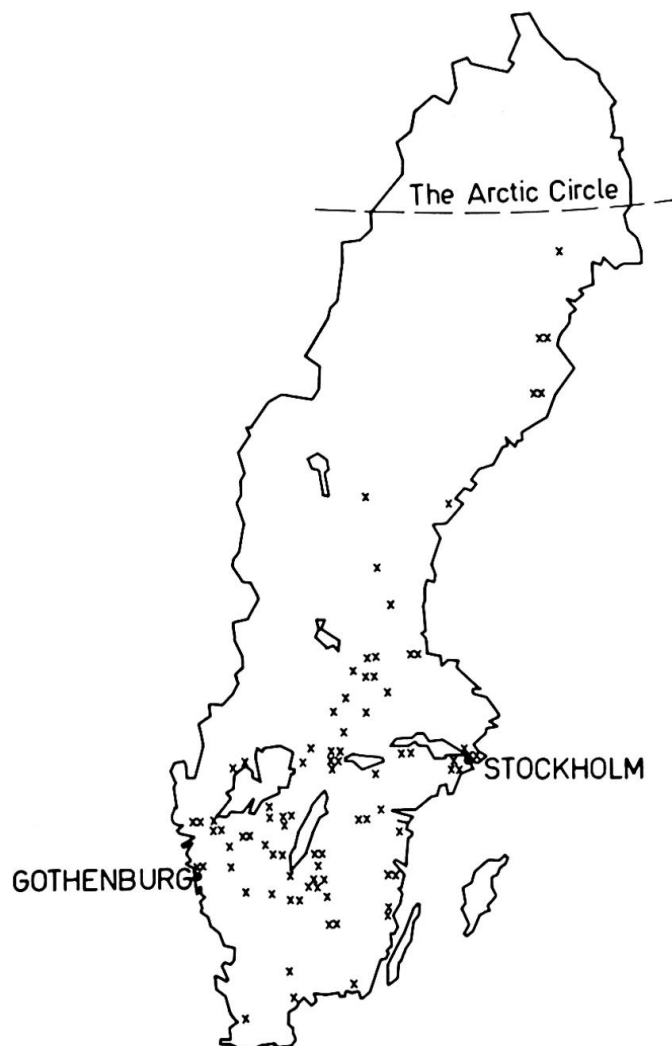
ZUSAMMENFASSUNG
Durch Schneelast verursachte Bauschäden werden behandelt. Fast einhundert Schäden sind untersucht worden, und einige Schadenfälle werden näher beschrieben. Die meisten beschädigten Konstruktionen sind leichte Konstruktionen aus Stahl oder Holz. Die Ursachen der Schäden sind gewöhnlicherweise Fehler beim Entwurf oder bei der Herstellung.

1. INTRODUCTION

During the winter 1976/77 heavy snow loads caused several structural failures in Sweden. Most of these failures occurred in the southern part of the country (Fig.1). The damages were of different types, ranging from failures in roof covering due to freezing water to completely collapsed buildings.

This investigation was concentrated on damaged structural members since failures of a member may often lead to complete failures of roofs or of buildings. In these cases there are great risks that people get hurt and the failures often lead to great losses in production etc. The aim of this investigation was to collect as much information as possible about the causes of the damages. Almost one hundred different damaged structures were studied.

During the winter the snow depth at different locations was measured by the Swedish Meteorological and Hydrological Institute (SMHI). Some of these measurements were compared with data from previous winters. It was found that in some cases the snow depth during the winter 76/77 considerably exceeded the 50 year Mean Recurrance Interval (MRI) ground snow depth, cf. table 1. However, this is not necessarily an extremely high value of the load.

SMHI-Station	Measured snow depth	50 year MRI
	m	m
Nyköping	0.75	0.66
Norrköping	0.74	0.51
Jönköping	0.69	0.38
Växjö	0.38	0.51
Ulricehamn	0.84	0.85
Skara	0.63	0.45
Falun	0.78	0.81

Fig.1   Map of Sweden with marked failure locations.

Table 1   Measured maximum snow depth and 50 year MRI ground snow depth.

2. COLLECTING INFORMATION

At first some information on damages was collected from notes in newspapers. In order to follow up these articles building approval authorities in all the 277 town and rural districts in Sweden were contacted and asked to report damages. The information obtained this way was of very varying quality. In addition to these "official" ways we got information through personal contacts with consulting engineers, contractors and insurance companies.

It was found that the first information either obtained by a letter or by phone was not always correct. A deeper study of a damage gave further details and revealed that the damage was not quite as firstly described and that the causes first assumed were not the proper ones. In roughly half of the cases studied we had to change our opinions. It is obviously necessary to treat first-hand informations with great care.

During the investigation of some failures it was apparent that some of the manufacturers were most unwilling to give any information about the building. They seemed to be afraid of getting a bad reputation.

3. CAUSES

The main reason for the structural failures has been the heavy snow loads causing the total load to exceed the load carrying capacity of the structure.

Table 2 shows a comparison of all the failures examined, with respect to both the cause of failure and the structural material. The table contains both small and big damages – ranging from buckling of steel sheets to total collapse of whole structures. The line in the table denoted *"Excessive snow load"* includes the cases where the amount of snow exceeded the snow load given by the Swedish Building Code and the cases with drift snow and sliding snow. *"Manufacturing faults"* includes all types of deviations from the prescribed design, both in the factory and at the building site. *"Underdesign"* means that mistakes were made either in the calculations or as an inappropriate design.

Estimated cause of failure	Steel %	Timber %	Aluminium %	Concrete %
Excessive snow load	23	15	1	1
Manufacturing faults	6	8	–	–
Underdesign	14	24	–	1
Other reasons	4	3	–	–
Total	47	50	1	2

Table 2   Examined failures, divided in causes of failure and structural material expressed as a percentage.

Often there have been many possible causes to the failure. The most probable cause in each case was counted in table 2, but sometimes alternative reasons might exist. Some failures were caused by a combination of reasons, e.g. damages on carports where sliding snow from an adjacent roof caused the structure to deflect horizontally; this structure was not designed for horizontal loads.

There are only a few measurements of the actual snow load on damaged buildings. This made it very difficult to decide in which cases excessive snow load was the prime cause of the failure. It is possible that we e.g. have stated "under-design" or any "other reason" for a structure that also was exposed to excessive snow loads. Drift snow loads have caused nearly 25% of all the failures. This is a remarkably high figure, especially when considering the fact that drifted snow was included already in the Swedish code of 1950. Table 2 shows that the failures mostly are caused by mistakes in the design or in the manufacturing. These failures include 64 per cent of the timber structures, 43 per cent of the steel structures and one concrete structure. This concrete damage was caused by a combination of underdesign and overload.

4. SOME TYPICAL STRUCTURAL FAILURES

Bad gluing of wooden structures has caused failures in glulam beams and plywood webbed I-beams. The glulam beams were of an I-type where the gluing of the flanges to the web was badly done. Due to the thickness of the flanges it was probably impossible to achieve a proper pressure along the whole gluelines during the manufacturing. One of the basic conditions for a successful gluing is that the glued surfaces are plane enough to come in close contact and that the applied pressure is sufficiently high. Especially in the case of nail-gluing it is a necessity to use planed surfaces. The plywood beams failed due to badly planed flanges resulting in bad glue joints.

Timber connections with *nail plates* (punched metal plates) are sensitive to mis-placements of the nail plates since the plate size often is small. Collapses of roof trusses were found to be due to too small nail plates at the heel joint. These small plates were placed so that cracks could develop in the rafter and then cause a collapse. When nail plates are used it is necessary not only to determine the minimum size of the plate but also to take into consideration the possibility for cracks to develop.
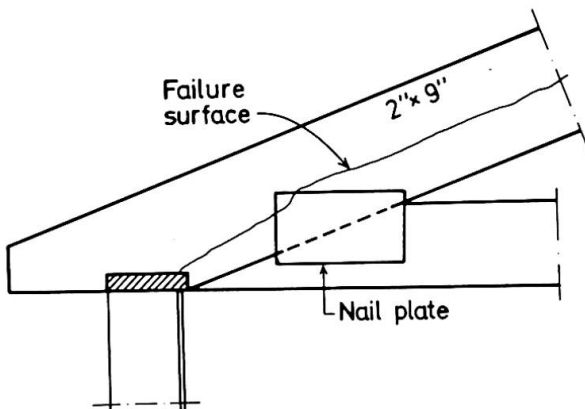

Fig.2 Heel joints with a too small nail plate.

Fig.3 Buckled Z-purlin.

Noninsulated buildings with light-weight steel trusses, covered with roofing
membranes or corrugated steel sheets, have been involved in several failures.
One of the reasons for this is that the buildings once were meant to be heated
and thus designed for a low snow load, due to the absence of heat insulation.
The use of the buildings has been changed and they were often used without
heating. This of course means that snow accumulates on the roof in an unexpec-
ted extent. Some of these buildings were also badly designed, which was the pri-
mary cause of failure.

Steel columns have been involved in some cases due to improper design. In one
case the building had no bracing so the buckling length was twice the column
length. A similar thing happened in a building where an additional building
was built and the old brick wall between the houses was taken away. In the ori-
ginal building the brick wall between the steel columns prevented lateral
buckling. By the removal of the lateral support the buckling load for the co-
lumn reduced drastically and the columns could not resist the snow load.

5. SPECIAL DAMAGES

5.1 Wood truss frame

This building was used as a cold storage. The primary structure was a three-
hinged wooden truss frame. After about 20 years of service in one place the
building was moved to another place. A drawing of one-half of the truss is shown
in Fig.4. The flanges in the truss-beam were made of two 2"×5". When the buil-
ding was moved the contractor cut the frames in the sections A-A (Fig.4). In
these joints lap splices of 2"×5" were nailed with just a few nails to each part.
The lengths of the lap splices were about 1 m.

The whole building collapsed due to failure in the joints A-A. Probably this
was a progressive failure starting in one frame. At failure the snow load was
estimated at 1.1 kN/m^2 based on in situ measurements. According to the Swedish
Building Code the joint in the tension flange should have been nailed with
about 130 nails. The estimated number of nails actually used in the joint corre-
spond to an *allowable* load of 0. kN/m^2 which is less than the dead load .4 kN/m.
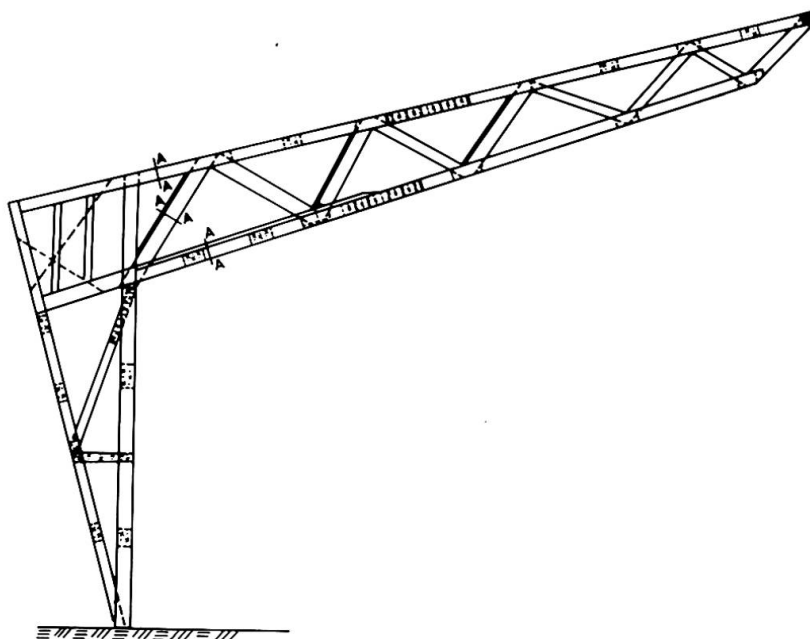0.3 kN/m^2. The total load at failure was estimated at 1.4 kN/m^2.

Fig.4 One half of a three-hinged truss frame, spanning 15.5 m, with joints at A-A.

5.2 Steel column

A storehouse 135×70 m^2 for sawn timber products was built in 1968. The height
was approximately 9 meters. The structure was a flat roof made of crossed milled
I-beams (beam depth ranging from 280 to 450 mm) resting on wide flange steel
columns. The columns were placed in a square net, 14×15 m^2. The façace columns
were HEB 180 and the others were HEB 200. The column length varied between 8
and 9.4 m. No diagonal bracing between roof and ground was used anywhere. At
the ground the columns were fixed in cast concrete.

The whole structure collapsed due to overall column buckling (Fig.5). The roof
snow depth was 0.55 m. The unit weight of snow varied between 2.6 and 2.9 kN/m^3
which means that the roof was subjected to a snow load of approximately
1.5 kN/m^2.

The column load caused by dead load and snow load was estimated at 360 kN.
Assuming Eulers *first* buckling case the column buckling load is 105 kN and the
slenderness ratio about 400. On the other hand the buckling load 360 kN corre-
sponds to the buckling length 1.08 times the column length. That is very close
to Eulers *second* buckling case. This means that the stiffness of the connections
between the columns and the roof girders have a certain influence on the buck-
ling load. It probably also means that the columns were bracing each other due
to smaller differences in loads etc.

This case is an example of a poor design. With diagonal bracings the collapse
should probably have been avoided.

Fig.5 Buckled columns.

5.3 Concrete structure

The failure occurred in a prefabricated concrete structure as a shear failure
at the supports of roof elements of a TT-type. The TT-element consisted of a
thin concrete plate with two separate webs. The elements were 2.4 m wide with
the span 15 m. The roof was divided in one higher and one lower part. Drift
snow accumulated on the lower part. This snow drift corresponded to a maximum
total load of about 9 kN/m^2 which was about 30 per cent higher than the pre-
scribed design load.

At the support the shear reinforcement in the web consisted of one ribbed rein-
forcement bar $\emptyset$ 16. The yield force in such a bar is about 80 kN. With a simple
equilibrium model for the forces at the support it was found that this corre-
sponds approximately to the load 7.9 kN/m^2 for the element in the worst position.
The reinforcement bar was actually yielding.

6. CONCLUSIONS

The snow damages have mainly occurred in light-weight structures like steel and
timber structures. These are often more sensitive to overload from live loads.
The heavy concrete structures are mostly very insensitive to variations in live
loads.

One reason for the damages is that drifted snow has not been properly conside-
red. In nearly 25 per cent of the cases drift snow has been involved. Other
causes are bad design and bad manufacturing of the structures which caused
more than 50 per cent of the failures.

One experience from this study is that it is difficult to rely on the informa-
tion you get. It is always necessary to cautiously use given information.

The failures investigated do not demand an increase of the design snow load.
Most of the failures had occurred even with an increased value of the design
snow load.

REFERENCES

JOHANNESSON, B., JOHANSSON, G., Snow damages during the winter 1976-77
    (in Swedish). Statens råd för byggnadsforskning, Stockholm.
    Rapport R15:1979.
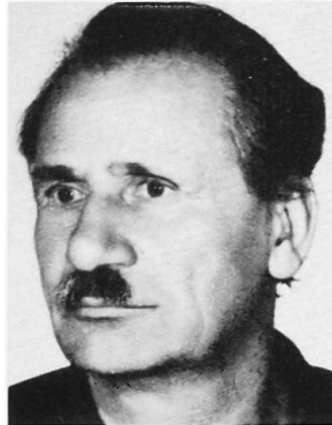
Leere Seite

Blank page

Page vide

Determination of Design Snow Loads

Détermination de la charge de neige

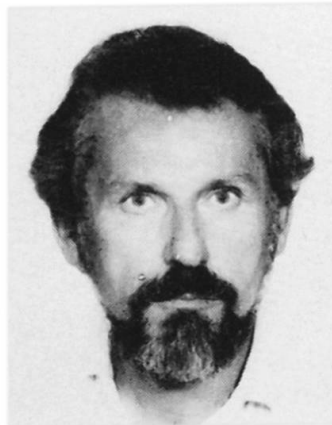Rechnerische Bestimmung der Schneelast

Vuk MILCIC
Prof. Dr.
University of Zagreb
Zagreb, Yugoslavia

Vuk Milcic, born in 1921, graduated and received his Sc.D. from the University of Zagreb. As a chief designer, he was in charge of an office for designing metal structures. Since 1973 he has held a chair for metal structures. Now, as head of the Department of Metal and Wooden Structures at the Faculty of Civil Engineering, Univ. of Zagreb, his major concern is the safety of metal structures.

Edo HEMERICH
Senior Lecturer
University of Zagreb
Zagreb, Yugoslavia

Edo Hemerich, born in 1940, graduated at the University of Zagreb. Employed at the Faculty of Civil Engineering since 1966 in the Department of Metal and Wooden Structures, Univ. of Zagreb, as technical manager of the department.

SUMMARY
Based on probabilistic methods, level II, the reliability of steel structures under snow loading has been investigated and a simple formula developed for estimating the snow load. By this means a more uniform degree of safety can be achieved under this loading condition.

RESUME
Une formule simple est proposée pour la détermination de la charge de neige. Elle résulte de recherches sur la fiabilité des structures, au moyen de la méthode probabiliste. Un degré de sécurité suffisant et plus uniforme est ainsi obtenu pour le dimensionnement des structures.

ZUSAMMENFASSUNG
Eine vereinfachte Beziehung für die rechnerische Bestimmung der Schneelast wurde hergeleitet. Sie basiert auf Forschungsergebnissen über die Sicherheit von vorwiegend durch Schnee belasteten Stahlbauten und wurde unter Verwendung probabilistischer Methoden erhalten. Die vereinfachte Beziehung ergibt einen genügenden und einheitlicheren Sicherheitsfaktor auch bei Anwendung der üblichen Verfahren mit globalen Sicherheitskoeffizienten.

1. INTRODUCTION

The problems of non-uniform safety degree of our bearing structures become distinctly revealed where snow is a predominant load. From experience, we know that light structures (of lesser weight but also with little dead load in general) suffer damages due to snow load much more frequently than other structures under other and bigger loads. Such structures are most often steel roofs or halls but they can also be wooden or light reinforced concrete structures. Although, most often in such cases, a direct cause of a collapse or of a damage in general can be found out as a consequence of an error commited in designing or construction, yet it is significant that similar errors on other structures do not result in such drastic consequences. The safety degree of predominantly snow loaded structures is obviously too low.

The solution of the problem of making the safety degree of bearing structures uniform was embarked upon about ten years ago on a wide international scale. As a result of the work of various international associations, general principles on achieving reliability and safety respectively of all bearing structures regardless of the material, the type or the way of stressing [1] and [2] have already been set up. Therefore, in future procedures of structural design, by introducing, on the semiprobabilistic basis, partial safety coefficients, and by virtue of statistical data of characteristic values of actions, it will be possible to equalize the safety degree for all structures regardless of the predominance of the action. But, in so far applied deterministic procedure with the global safety coefficient and prescribed nominal calculation values for actions, this non-uniformity remains present almost always on the side of the lower safety in case of predominant snow load.

In the course of 1980, at the Faculty of Civil Engineering, University of Zagreb, a research project to determine the safety degree of predominantly snow loaded steel structures in SR Croatia, Yugoslavia, has been realized by establishing the reliability index by means of the level II probabilistic method in the Hasofer-Lind procedure [3]. Based on the analysis of the results, the conclusion was drawn that the safety degrees achieved at various locations were highly non-uniform, and considering ratio of the dead load to the snow load, almost always on the side of lower safety.

This statement prompted further research to find out the necessary calculation snow load by means of which even now the safety degree could be equalized in locations with regard to various statistical data about snowfall as well as with regard to different relations between the dead load and the snow load. As a result of the work and of the data obtained from the analysis of the reliability index of existing structures, a simple formula for the necessary calculation snow load has been found out in the structural designing procedure by currently standard method with the global safety coefficient.

2. BASIS FOR FORMULA DERIVATION

As a primary basis for the derivation of this formula, a linear equation of the ultimate limit state from the probabilistic procedure of the level II method was taken.
Taking into consideration only structures in which snow is a predominant load, only three basic variables as random values were chosen. These are resistance, dead load and variable live load.
Equation of ultimate limit state in the probabilistic level II is:

$$X_R^* - X_D^* - X_L^* = \emptyset$$

Indexes: R ... structure resistance
D ... dead load
L ... variable live load (snow)

in wich

X_i ... any of the basic variables as random value (i=R,D,L) expressed as a
force,

and its design value in checking point i.e. the one that, according to the
Hasofer-Lind procedure, corresponds to the greatest probability of failure

$$X_i^* = m_i \cdot (1 - \alpha_i \cdot \beta \cdot V_i)$$

in which

m_i ... mean value of basic variable (i=R,D,L)
α_i ... sensitivity coefficient of basic variable (i=R,D,L)
V_i ... coefficient of variation of basic variable (i=R,D,L)
β ... reliability index, the value of which is chosen with regard to the
adopted safety degree

In order to reduce this equation of ultimate limit state of the probabilistic
level II to the probabilistic level I, it is necessary only to introduce

$$X_i^* = \gamma_i \cdot X_i^k \qquad \text{for} \quad i = R,D,L$$

in which

$X_i^k =$ ... nominal (characteristic) value of the basic variable from the deter-
ministic procedure of design (i=R,D,L)

$$\gamma_i = \frac{m_i \cdot (1 - \alpha_i \cdot \beta \cdot V_i)}{X_i^k} \quad \text{... partial safety coefficient for the basic variable}$$
(i=R,D,L)

In the current deterministic procedure of the bearing capacity proof with the
global safety coefficient the linear equation of ultimate limite state is as
follows

$$X_R^k = \gamma_N \cdot (X_D^k + X_L^k)$$

in which

γ_N ... global safety coefficient is standardized in current deterministic
design procedure

The equation of the ultimate limit state of probabilistic level I can be trans-
formed into

$$X_R^k = \frac{\gamma_D}{\gamma_R} \cdot X_D^k + \frac{\gamma_L}{\gamma_R} \cdot X_L^k$$

if

$$\kappa = \frac{X_D^k}{X_L^k}$$

is inserted

$$X_R^k = \frac{\gamma_D}{\gamma_R} \cdot \kappa \cdot X_L^k + \frac{\gamma_L}{\gamma_R} \cdot X_L^k = X_L^k \cdot \left(\frac{\gamma_D}{\gamma_R} \cdot \kappa + \frac{\gamma_L}{\gamma_R} \right)$$

is obtained.

Formally, we reduce this equation to the form similar to the deterministic one

$$X_R^k = \gamma_N \cdot X_D^k - \lambda_N \cdot X_D^k + X_L^k \cdot \left(\frac{\gamma_D}{\gamma_R} \cdot \mathcal{K} + \frac{\gamma_L}{\gamma_R}\right)$$

$$X_R^k = \gamma_N \cdot X_D^k - \gamma_N \cdot \mathcal{K} \cdot X_L^k + X_L^k \cdot \left(\frac{\gamma_D}{\gamma_R} \cdot \mathcal{K} + \frac{\gamma_L}{\gamma_R}\right)$$

$$X_R^k = \gamma_N \cdot \left[X_D^k + X_L^k \cdot \underbrace{\left(\frac{\gamma_D}{\gamma_N \cdot \gamma_R} \cdot \mathcal{K} + \frac{\gamma_L}{\gamma_N \cdot \gamma_R} - \mathcal{K}\right)}_{\eta} \right]$$

which yields the final expression

$$X_R^k = \gamma_N \cdot (X_D^k + X_L^k \cdot \eta)$$

As is evident, if in the current equation of the ultimate limit state of the deterministic procedure only the corrected value of the predominant load (snow in our case) is introduced, the required safety degree of a structure can be obtained. This value for the correction coefficient is

$$\eta = \frac{\gamma_L}{\gamma_N \cdot \gamma_R} + \mathcal{K} \cdot \left(\frac{\gamma_D}{\gamma_N \cdot \gamma_R} - 1\right)$$

This means that the new calculation value for the predominant variable load (snow in our case) must be

$$X_o^k = \eta \cdot X_L^k = \left[\frac{\gamma_L}{\gamma_N \cdot \gamma_R} + \mathcal{K} \cdot \left(\frac{\gamma_D}{\gamma_N \cdot \gamma_R} - 1\right)\right] \cdot X_L^k$$

By introducing the values for γ_L and for $\mathcal{K}$ the general expression is obtained

$$X_o^k = \frac{m_L}{\gamma_N \cdot \gamma_R} (1 + \beta \cdot \alpha_L \cdot V_L) + X_D^k \cdot \left(\frac{\gamma_D}{\gamma_N \cdot \gamma_R} - 1\right) \dots \dots \quad (1)$$

in which X_L^k value is eliminated.

3. FORMULA DERIVATION FOR SNOW

If the mentioned general expression (1) is applied to determine the necessary calculation snow load ($X_o^k = S$) in order to obtain a sufficient and uniform safety degree of a structure, a series of parameters must be determined in this formula. These are primarily the mean value (m_L) and the coefficient of variation (V_L) which refer to the snow load as a random variable connected to other variables through the serisitivity factor (α_L). Then the partial safety coefficient for resistance (γ_R) and for the dead load (γ_D) must be determined as well as the characteristic value for the dead load (X_D^k). It is also necessary to choose the safety degree of a structure by accepting a certain reliability index (β) and to introduce into the formula the global safety coefficient (γ_N) which is prescribed in the current deterministic procedure of structural design. This is a very large number of parameters and, generally, the determination of calculation snow load could be a very complex task. Fortunately, for most of these

parameters some fixed values can be adopted. The analyses of results obtained
in the research work mentioned in the introduction, showed that changes of some
of the coefficients (γ_R, γ_D, α_L) run within very narrow limits: for γ_R from
1.09 to 1.14; for γ_D from 1.05 to 1.08 and for α_L from 0.805 to 0.899. Some
fixed values such as the ones for γ_R=1.10; for γ_D=1.07 and for α_L=0.86 can be
adopted so that this has almost not any substantial influence upon the value
of the final result. For the global safety coefficient we can choose the fixed
value of γ_N=1.5 which, in the current regulations, is the most frequently
used safety coefficient for steel structures with which only snow can be a dis-
tinctly predominant load. The choice of reliability index, by means of which a
sufficient safety degree is achieved, is a particular problem. The previously
mentioned analyses of results of the research work showed that the uniformity
of the safety degree for structures predominantly loaded with snow should be
made on the value β=4.0, which generally meets the requirements for the ulti-
mate limit state. As a characteristic value of the dead load there can be ta-
ken the nominal value of the covering usual with steel structures (X_D^k = G) and
this possibly with two variants: as a light covering (i.e. G_1=300 N/mm^2) and
as a heavy covering (i.e. G_2 = 1000 N/mm^2).

Therefore, the remaining problem is to determine, from statistical data about
snowfall, the mean value of snow loads on a roof (m_L) as random values during
the life period of a structure (n-years), and to find out the corresponding
coefficient of variation (V_L) for this random value. This coefficient of vari-
ation is corrected, in order to use the Hasofer-Lind method, considering the
reduction of the real distribution of the extreme snow load to the necessary
normal distribution, according to the simplified Paloheimo-Hannus procedure (4).

If we know the maximum annual ground snow weight (Q_i) recorded for years (T=10
to 30 years), then we can calculate the mean value from

$$\overline{Q} = \frac{\sum Q_i}{T}$$

and also the standard deviation (s) from

$$s = \sqrt{\frac{\sum (Q_i - \overline{Q})^2}{T}}$$

We can possibly correct this standard deviation by way of one of the known pro-
cedures due to the relatively small number of members of the set Q_1.

On the usual assumption that the distribution of maximum annual snow weights
follows the Type Ex-I, we can also calculate the mean value of the extreme snow
weights ($\overline{Q_n}$) during the life period of a structure (n-years) from

$$\overline{Q_n} = \overline{Q} + \frac{\sqrt{6}}{\pi} \cdot s \cdot \ln(n)$$

and the coefficient of variation (V_n) from

$$V_n = \frac{s}{\overline{Q}_n} = \frac{s}{\overline{Q}+ \frac{\sqrt{6}}{\pi}.s.\ln(n)}$$

For the snow load on a flat roof, it is necessary to reduce the ground snow weight with the empiric coefficient of 0.8 and so the mean value is obtained.

$$m_L = 0.8 . (\overline{Q} + \frac{\sqrt{6}}{\pi}.s.\ln (n)) \tag{2}$$

The coeficient of variation (V_n), in order to reduce the distribution Type Ex-I to the normal distribution, should be reduced by means of

$$V_L = V_n . \frac{\beta_{Ex-I}}{\beta_N} = \frac{s}{\overline{Q}+ \frac{\sqrt{6}}{\pi}.s.\ln(n)} . \frac{\beta_{Ex-I}}{\beta_N} \tag{3}$$

in which β_{Ex-I} is the reliability index of the Type Ex-I distribution for the same probability which corresponds to the β_N reliability index for the normal distribution.

It is also necessary to adopt a particular life period of a building, expressed in years. As warehouse and industrial halls with light steel bearing structures tend to be the most sensitive to the snow load, we can adopt their average life period which is about 30 years (n=30). To the already previously adopted reliability index $\beta = \beta_N = 4.0$, on the assumption of the same probability of failure, corresponds $\beta_{Ex-I} = 7.7$.

Therefore, determined are the values for all parameters by means of which a simple expression for calculation snow load $(X_o^k = S)$ of bearing structures can be obtained from the equation (1).

4. FORMULA FOR CALCULATION SNOW LOAD

In the equation (1) it is necessary to replace m_L by the expression (2) and to introduce all the above chosen fixed values for parameters ($\gamma_N = 1.5$; $\gamma_R = 1.1$; $\gamma_D = 1.07$; $\alpha_L = 0.86$; $\beta = 4.0$; n=30) the nominal value $(X_D^k = G)$ for the dead load so as to obtain a simple formula for the necessary calculation snow load $(X_o^k = S)$ on a flat roof

$$S = 0.485 . (\overline{Q}+2.65.s).(1+3.44.V_L)-0.35.G$$

The value for the corrected coefficient of variation (V_L) is obtained form (3) also by inserting the values for the fixed parameters (n=30; $\beta_{Ex-I} = 7.7$; $\beta_N = 4.0$)

$$V_L = \frac{1.925 . s}{\overline{Q}+2.65 .s}$$

For the value of the dead load (G) it is sufficient to take only two extreme cases

$G = 300$ N/mm^2 ..... light covering

$G = 1000$ N/mm^2 ..... heavy covering

and in very extreme snow loads the dead load can be neglected (G=0).
From the statistical data about snowfall it is necessary to calculate.

$$\bar{Q} = \frac{\sum Q_i}{T}$$ ... mean value of recorded maximum (Q_i) annual ground snow loads

(T is 10 to 30 years)

$$s = \sqrt{\frac{\sum (Q_i - \bar{Q})^2}{T}}$$ standard deviation of maximum annual ground snow loads

In the current deterministic design procedure with global coefficient of safety, most often by the allowable stress method, these values for the calculation snow load can be used not only for the predominantly snow loaded structures but for all structures, because these values are then always on the safe side and this does not have any influence upon the economy of a building.

5. BIBLIOGRAPHY

[1] ICSS: General Principles on Reliability for Structural Design, Report IABSE, Volume 35/IV-1981.

[2] CEB-FIB: Common Unified Rules for Different Types of Construction and Material, Bulletin d'information N° 116-D, Paris 1976.

[3] HASOFER, A.M.; LIND,N.C.: An Exact and Invariant First-Order Reliability Format, Journal of the Engineering Mechanics Division, ASCE, Volume 100, No EM1, pp. 111-121/1974.

[4] PALOHEIMO,E.; HANNUS,M.: Structural Design Based on Weighted Fractiles, Journal of Structural Division, July 1974. pp. 1367-1378.

Leere Seite

Blank page

Page vide

Cable-Suspended Pipeline Crossing a Glacier in the Alps

Conduite suspendue au dessus d'un glacier dans les Alpes

Hängeleitung über einen Gletscher in den Alpen

Josef GROB
Civil Engineer
Universal Eng. Corp. (UEC)
Basle, Switzerland

Josef Grob, born in 1945, obtained his civil engineering and his doctorate degrees at the Swiss Federal Institute of Technology in Zurich (ETHZ). He has been working as a senior designer with the consultants Schneller, Schmidhalter and Ritz, Brig, Switzerland. At present he is a division manager in structural and civil engineering with UEC.

SUMMARY

A four stage pump installation supplies water to a site at Felskinn above Saas-Fee, Switzerland, from 1830 to 2987 m above msl. At the top stage the water pipeline is suspended across a glacier by a free hanging cable system with a main free span of more than 600 m. It was necessary to erect an intermediate pylon on the glacier, due to the unfavourable characteristics of the topography. This pylon moves about 15 to 20 m per year as a result of the creep of the glacier.

RESUME

Un système d'approvisionnement en eau, équipé de 4 stations de pompage, alimente un chantier situé à Felskinn, au-dessus de Saas-Fee en Suisse, soit entre les altitudes de 1830 et 2987 m. La section supérieure de cette conduite d'eau traverse un glacier et est suspendue sur une portée principale de plus de 600 m, grâce à un système de câbles. La topographie défavorable a contraint la mise en place d'un mât intermédiaire dont le déplacement annuel atteint entre 15 et 20 m par an à la suite du mouvement du glacier.

ZUSAMMENFASSUNG

Zur Versorgung einer Baustelle auf Felskinn oberhalb Saas-Fee in der Schweiz transportiert eine vierstufige Pumpförderanlage Wasser von 1830 auf 2987 m.ü.M. Die Förderleitung überquert im obersten Abschnitt einen Gletscher an einer Freileitung mit einer Hauptspannweite von über 600 m. Wegen des ungünstigen Längenprofils musste auf dem Gletscher eine Mittelstütze angeordnet werden, die sich infolge der Kriechbewegungen des Gletschers um 15 bis 20 m pro Jahr verschiebt.

1. INTRODUCTION

The cable-suspended pipeline, Fig. 1, is part of a pumping installation for the supply of water to the site of the construction of an underground cable-car "Metro-Alpin" at Saas-Fee, Switzerland. The pipeline supplies water from a point 1830 m above msl to Felskinn at an altitude of 2987 m.

The "Metro-Alpin" is the biggest construction project of the company Luft-seilbahnen Saas-Fee AG and was started on 1st September 1981. The cable-hauled cars running on rail in the tunnel provide access to a large glacial tourist aera above Saas-Fee. This system was chosen instead of a suspended cable-car for ease of maintenance and operation and from environmental considerations. The cars run in an inclined tunnel 1447 m long to provide a connection from Felskinn which is reached by a suspended cable-car built in 1969 to the Mittelallalin shoulder at 3456 m above msl.

The inclined cable-car gallery runs partially under glacier with a minimum rock cover of 10 to 15 m. For this reason careful excavation methods by mechanical means were chosen, in spite of the bigger logistical problems. Conventional drill an blast methods would hardly have been feasible. The tunnel profile has a diameter of 420 cm and was driven by a Robbins tunnelling machine type 136-204. This machine was transported in several parts of not more than 12 t weight to the tunnel starting point at Felskinn using the existing suspended cable-car.

The client arranged to supply the site with a maximum daily water quantity of 100 m3 for the free use of the contractor. The contractor had to re-cycle the water several times due to the limited quantity available. Economic considerations for the design of the 100 m3/day (~1.25 l/sec) pumping installation led to a layout of four pumps in series. At the top stage the pressure head reaches 327 m consisting of 302.6 m level difference and 24.4 m friction losses.

Fig. 1 Cable-suspended pipeline

The siting of the pipeline and the intermediate reservoirs was determined by geotechnical and topographical conditions and potential avalanche areas also had to be avoided. For the lower stage the pipeline lies in soft ground having some vegetation. Above 2100 m there is no vegetation in the glacial moraine zone and finally the pipeline crosses a glacier between reservoir No. 4 and Felskinn. This glacier creeps between 15 and 20 m per year and obviously the pipeline cannot be embedded in such a movement zone. Therefore the pipeline crossing the glacier is suspended on a free-hanging cable system, Fig. 1.

The costs for the pumping installation of total length 3950 m and elevation of 1160 m are about 1.6 m SFr. of which about 50 % forms the cost for the 910 m long suspended section.

2. SUSPENDED PIPELINE SECTION

The suspended pipeline section has no stiffening leg. The water pipeline is encased in an outside hard polyethylene pipe of 125 mm diameter which is suspended from two cables each 36 mm diameter. The suspension cables are fixed at both ends, at the bottom end on a steel tripod 12.5 m high and at the top end to a concrete bollard giving a means to adjust the cable tension if required. The tripod is placed at Reservoir No. 4 on a moraine layer of 12 m depth lying on old stationary ice. It is anchored into the moraine layer with 4 x 40 t ground anchors to provide stability against overturning. The moraine layer is a permafrost zone except for the surface. At the top end the cables are fixed to a concrete bollard which is anchored with 2 x 40 t ground anchors into the serpentine rock which is also a permafrost zone.
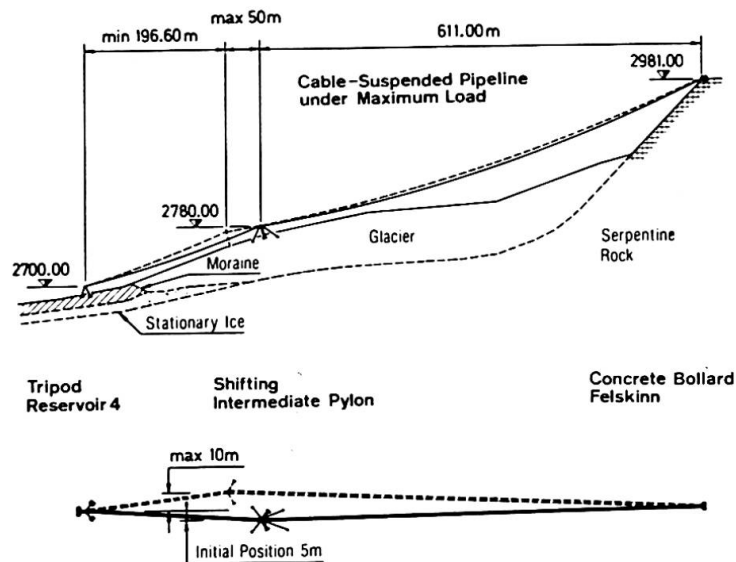

Fig. 2   Suspended pipeline section

Due to the unfavourable surface profile of the glacier and the levels of the anchorage points, see Fig. 2, an intermediate pylon was necessary. The head of this 35 m high pylon is restrained by four cable stays anchored in the glacier. This intermediate pylon is moving downhill with the glacier resulting in a relative displacement from the supported cables which move through saddles at the head of the pylon. The surface creep of the glacier is about 15 to 20 m per year and the system allows a maximum displacement of the intermediate pylon of 50 m longitudinally and ± 10 m in the tranverse direction. With this arrangement an uninterrupted water supply to the construction site is possible. The total time of construction of the "Metro-Alpin" is 3 years to completion for the 1984-85 winter saeson. The initial position for the pylon transversally was given by the actual direction of creep and by the position of a crevasse.

The capacity of the pumping installation will only be used partially after the end of the construction of the underground cable-car for the supply of drinking water. Therefore at this time an interruption in the water supply is

acceptable due to the lower water demand and the removal of the inter-
mediate pylon and its re-erection in the initial position can be
accomodated. This will be the case after reaching a longitudinal displacement
of 50 m or a transverse displacement of 10 m. The two free spans thus vary
from: lower span 246.6 m to 196.6 m
        upper span 611.0 m to 661.0 m

The problem of freezing in the pipeline is solved by keeping the water
moving all the time and emptying the pipeline whenever pumping is stopped.
This is guaranteed by a minimum slope of the pipeline of 10 %. Additionally
at the outlet from Reservoir No. 4 below the most exposed suspended section,
the water may be heated using a 25 kW heater to raise the temperature 5°C.
In practice it is found that even with very low temperatures the water
normally requires no supplementary heating due to the solar energy absorbed
by the black hard polyethylene pipe.

3. SUSPENDED SYSTEM

3.1 Construction

The main load bearing elements of the suspended system consist of two 36 mm
diamter "Seale" multi-tendon cables with a fibre core. The guaranteed
tensile strength of each cable is 810 kN.
At 254 cm centres a rectangular steel pipe section, 60 mm x 40 mm, is fixed
across the two cables which are 100 cm apart. From this is hung the hard
polyethylene pipe with two steel cables, Fig. 3.

The main steel cables and the polyethylene pipe have very different
longitudinal deformations. In order to avoid forces in the polyethylene pipe
the 501 cm long sections are not fixed together at the spigot and socket-
type joints. On the assumption that the friction at the joints will vary a
sliding clamp arrangement, see Fig. 3, is provided at each joint to prevent
the pipe sections pulling apart. This consists of two clamps joined by a
slotted steel strap to allow 160 mm of movement.
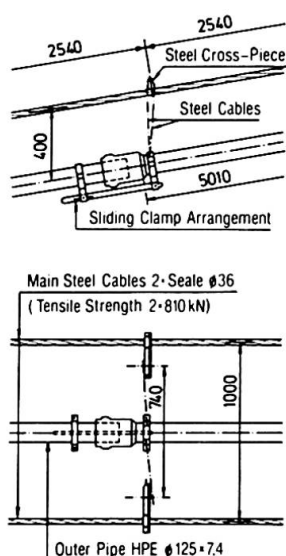

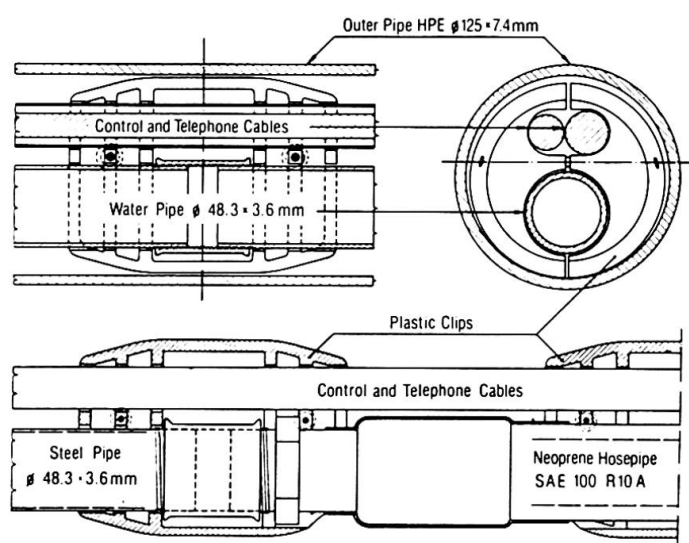Fig. 3 Suspended system   Fig. 4   Internal pipe and cable bundle

The outer polyethylene pipe protects the water pipe and also carries one telephone and one control cable, Fig. 4. This pipe minimises the ice load due to its smooth surface and provides an internal air space which gives good temperature insulation. Polyethylene material is used because of its ductility and because the added carbon black gives good resistance to utra-violet light.

The suspended system has large deformations under wind and ice loads and temperature differences. The internal pipe and cable bundle is free to move along the whole length of the suspended section. This avoids forces due to these deformations and to the temperature difference usually existing between the water pipe and the suspension cables. The internal bundle is clamped only at the top end. The maximum relative displacement between the outer pipe and the bundle is reached at the lower tripod end and is compensated by a special articulated sliding construction.

The water pipe and cable bundle is held together every 2.5 to 3 m with specially designed plastic clips, Fig. 4, which locate the steel pipe and cables in the designated position and facilitate the pulling process in the erection phase. This solution also gives a better temperature insulation of the water pipe because there is no direct contact between the water pipe and the external pipe.

A steel pipe with screwed joints, 48.3 mm external diameter, 3.6 mm wall thickness, is used for most of the water line. In sections of tight curvature flexible high pressure neoprene hosepipe type SAE 100R 10A is chosen. This was the case near both anchorage points and at the intermediate pylon. The neoprene hose at the top end is reinforced with a special tension member consisting of two small steel cables to provide additional tensile strength for the holding force of 20 kN at this point.

3.2 Design

The load assumptions were basically taken from the Swiss Code SIA 160 (1970) and adapted to the local conditions.
The total design loads on the suspended system are:

Dead load including water   0.21 kN/m

Quasi-statical wind load   0.25 kN/m

Ice load   0.26 kN/m

The calculation of the tensile forces and cable deformations was carried out for the above loads in a temperature range of -30°C to 20°C. The elasticity theory 3rd order was used for the computation for the final state as well as for the different construction stages.

The friction effects at the cable saddles were calculated by trial and error methods. The Young's modulus of the "Seale" multi-tendon suspension cables with fibre core was assumed to the constant at 90 kN/mm2 over the occurring stress range. For the case of the maximum shift of the intermediate pylon the statical calculation gave the following values:

Max. vertical load: max. tensile force: 504 kN/cable

                        max. sag: 29.8 m

Dead load and wind: max. tensile force: 403 kN/cable

                        max. sag: 15.8 m

                        max. horizontal deformation: 18.8 m

These figures show that the dead load + wind case is not governing the design
of the suspended construction. Even considering the dynamic behavior with the
lowest frequency of 0.80 Hz in the bigger span the tensile forces in the cables
due to dead load + wind are less than the forces due to the maximum vertical
load. Thus a minimum theoretical safety factor of 810 kN/504 kN = 1.61 is
obtained against failure of the cross-section of the cables.

4. PYLONS

4.1 Intermediate Pylon

The intermediate pylon, Fig. 5, constructed of Fe 360 steel has two legs
of 27.02 m and 35.50 m length. The head of this pylon is restrained by steel
cable stays anchored in the glacier. Since the creep deformations under the
two legs will not be exactly the same the legs are linked at the head with
an articulated connection so that the feet can have a maximum displacement
relative to each other of ±3m. The legs are supported on steel plate footings
and are articulated in both directions. Timber railway sleepers are placed
under the steel baseplates in order to prevent heat conduction into the ice
and thus excessive settlement. No other fixing is made, the pylon being held
down by the four cable stays and the vertical load on the construction.

Fig. 5 Intermediate pylon

Fig. 6   Head of intermediate pylon

Both legs are rectangular trusses, one 100 x 100 cm, the other 100 x 160 cm.
The shorter leg has a greater truss depth in order to carry the horizontal
forces from the cable saddles and the resulting bending moments. The
assembly carrying the two cable saddles is suspended at the head by four steel
cables, Fig. 6. This allows the assembly to be easily raised or lowered
together with the suspension cables. The saddles can rotate about two axes and
are kept in position laterally by a horizontal support frame.

4.2 Tripod

The tripod at Reservoir No. 4 is a 12.5 m high construction of Fe 360 steel consisting of two compression legs joined to form a triangular truss and a tension leg, Fig. 7. Two steel sections IPE 450 form the compression members of the truss and are 800 cm apart at the bottom and 100 cm at the top. The tension leg consists of two parallel steel sections HEA 220, 100 cm apart, embedded in a concrete footing with a steel cross-piece.

In the suspended section the water pipe and cable bundle slides in the external plastic pipe to give a theoretical relative displacement of up to 330 cm at the tripod under wind and ice loads and temperature differences. From safety considerations the special Z-shaped sliding construction, Fig. 7, allows a displacement of up to 400 cm. It is supported by a secondary steel structure connected to the tripod, Fig. 7. The relative displacement is taken by the curvature of the water pipe and cable bundle at the two corners of the Z-shaped sliding construction without any longitudinal strain. The curvature zones are a 4o cm long section at the top corner and a 530 cm long section at the bottom corner, the latter being protected by a concrete box enclosure. The telephone and control cables are flexible enough for these curves but for the water pipe special flexible "Anaconda" metal hoses with a 39 bar working pressure are used.

Fig. 7 Tripod at reservoir No. 4

Outside the concrete enclosure the water pipe and cable bundle is protected by specially designed plastic pipe sections as follows:

- sliding sections consisting of two concentric hard polyethylene pipes of diameters 125 mm and 160 mm in the top and vertical legs of the special sliding construction.
- articulated pipe-support on top of the concrete enclosure.
- hinged construction under the top corner taking tensile forces. It is connected to a support cross-piece which slides on both upper steel beams

of the secondary support structure.

5. ERECTION

Felskinn is the only site location having access by the existing cable-car.
The sites of the intermediate pylon and the lower tripod had to be supplied
using helicopters. Therefore the erection of the suspended construction in
the following steps was carried out from Felskinn wherever possible:

1. Erection of the lower tripod and intermediate pylon - maximum weight of
   prefabricated steel sections limited to 750 kg for helicopter transport.

2. Pulling and tensioning of the suspension cables in the half-raised
   position at the intermediate pylon.

3. Assembly and lowering of the outer plastic pipe and its support members
   by means of a temporary cable clamped at each suspension point.

4. Assembly of the water pipe and cable bundle and introduction into the outer
   plastic pipe.

5. Lifting and fixing of the cable saddles into their final position at the
   intermediate pylon.

6. Tension check and eventual correction of the tensile force in the suspension
   cables at Felskinn.

7. Assembly of the sliding construction at the tripod.

8. Clamping of the steel cross bars onto the suspension cables and removal
   of the temporary cable.

9. Sliding check of the water pipe and cable bundle by pulling it back
   into the initial position and clamping it at the top end.

The Felskinn cable-suspended pipeline had to be erected in winter under
sometimes very extreme conditions. The erection took place between October 81
and February 82 with some interruptions due to very bad weather.

REFERENCE

GROB J. / SCHNELLER P., Freileitung für die Wasserversorgung einer Baustelle
im Hochgebirge (Cable-Suspended Pipeline for the Water Supply of a Site in
the High Mountains), Baingenieur 11 - 17/1983.

Interaction of Wind with the Ice-Covered Structural Members

Effets du vent sur des éléments de structures recouvertes de glace

Wirkung des Windes auf vereiste Bauteile

Michael KAZAKEVITCH
Dr. techn. sciences
Gosstroy USSR
Dniepropetrovsk, USSR

Michael Kazakevitch, born 1939. For 15 years he was involved in problems of dynamics, aerodynamics and theory of oscillation damping of elastic structures. He is now employed as chief engineer in Dnieprprojectstal Constructsia Institute.

Igor GRAFSKY
Lecturer
Dniepropetrovsk State Univ.
Dniepropetrovsk, USSR

Igor Grafsky, born 1936. For 6 years he was involved in problems of experimental aerodynamics of blunt bodies. Now Igor Grafsky is lecturer at the Aero-Hydrodynamics Department of Dniepropetrovsk State University.

SUMMARY

In the paper, the following problems are investigated: the nature of the flowaround and the aerodynamic characteristics wind/loads of different ice-covered structure models as a function of the wind flow velocity, angle of attack and the degree of its turbulence. The types of ice-covered models were chosen because of the analysis of the real ice-rimmed accretion forms on the structural members corresponding to the physical process of their formation.

RESUME

L'écoulement et les propriétés aérodynamiques de différents modèles de structures couvertes de glace sont étudiés en fonction de la vitesse du courant d'air, de l'angle d'attaque et du degré de la turbulence. Le choix des types de modèles recouverts de glace est réalisé à partir de l'étude des formes réelles des concentrations de givre et de glace sur les éléments de construction, en correspondance avec le processus physique de leur formation.

ZUSAMMENFASSUNG

Es werden das Umströmungsverhalten und die aerodynamischen Eigenschaften verschiedener Modelle vereister Konstruktionen untersucht, die von der Geschwindigkeit des Windstromes, der Angriffsrichtung und dem Grade der Turbulenz abhängig sind. Die Auswahl der Modelle erfolgte aufgrund eines Studiums von in der Wirklichkeit vorkommenden Bauteilen, die mit Eis oder Rauhreif beschlagen sind.

1. INTRODUCTION

The aeroelastic instability of the bearing structural members of constructions, machine building structures communication lines, power transmissions and antenna systems takes place due to the formation of the ice-rimed accretion during the desposition and freezing of the overcooled water drops in the rain, fog or wet snow medium at the sublimation of water steam. The origin of such formations is caused by the interaction of the wind flow with the ice-covered structural members. This phenomenon is investigated in the given paper.

In this paper the following problems were investigated: the nature of the flow-round and aerodynamic characteristics (wind loads) of different ice-covered structure models depending on the wind flow velocity, angle of attack and the degree of its turbulence. The types of ice-covered models were chosen due to the analysis of the real ice-rimed accretion forms on the structural members in relation to the physical process of their formation.

2. THE SELECTION OF MODELS

2.1. The grounds

The analysis of ice-rimed accretion forms on the structural members and their generalization gave opportunity to choose four types of ice-rimed accretion models which are the most characteristic and which differ in geometrical dimensions (elongation of cross-section form) and in texture (Fig. I). These qualities of the models are caused by the physical processes of ice-rimed accretion formation.

The type of ice-rimed accretion depends on the size of the drops, velocity of their freezing in the moment of the contact with structural members and on the location of the constructions and their neighbourhood to the water reservoirs. At the deposition of large drops the freezing is going on slowly at the temperature close to zero centigrade. Large drops have time to spread over a surface and to form smooth water film, frozen in the form of the smooth ice deposit-glaze. Due to the observed data of the Applied Climatology Department of the Vojejkov Central Geophy-sical Observatory, the glaze [1] appears at the temperature of the air 0... -3°C. As a rule, such type of deposit is observed on the horisontal and sloping members. The shape (geometry) of the deposit is characterized by the velocity of the freezing and formation of glaze. It is reflected in the dimensions of three first models.

The fourth model corresponds to the formation of ice deposit when freezing of the small drops without their spreading over the surface. The air bubbles remain between the freezing pieces of ice-drops, therefore the ice surface is rough, with separate bulges and grooves. The glaze deposits, formed during the sticking of wet snow, have the same texture. These types of deposits are characteristic not only for horisontal or sloping but also for vertical members.

2.2. The geometrical characteristics of models

The models are made of foam plastic and covered with nitrocellu-
lose enamel. Their geometrical parameters are given in the
Table 1.

NN of models	Chord b, mm	Cross size, d, mm	Centre position X_T mm	Section elongation character-istic $\bar{c} = d/b$	Lower edge radius Rmm
1	62,5	50	25	0,8	16
2	75	50	25	0,67	9
3	110	52	26	0,47	6
4	120	46	30	0,38	2

Table 1   The geometrical parameters of models

Models of the length l = 400 mm are supplied by the end plates
which provide their two-dimensional wind flow.

3. THE EXPERIMENTAL TESTS

3.1 The aerodynamic loads

The aerodynamic drag coefficient C_x, lift coefficient C_y and
longitudinal moment m_z are received by the weight method by means
of measurement of the corresponding aerodynamic forces X, Y, M_z
by three-dimensional strain-measuring device:

$$C_x = \frac{X}{q\,S}\;;\qquad c_y = \frac{Y}{q\,S}\;;\qquad m_z = \frac{M_z}{q\,S\,\ell}\;,$$

where q – velocity head, $q = \rho V^2/2$; S – model characteristic
area, $S = \ell \cdot \ell$; ℓ – model chord; ρ – air tightness. The wind tun-
nel tests were carried out at flow velocities V = 10... 40 m/sec.
The corresponding Reynolds numbers are Re = (0,4... 2,6)$\cdot 10^5$. The
angle of attack changed in the range α = 0... 180°; turbulence
intensity changed in the range $\mathcal{E}$ = 0,5... 8%.

3.2 The influence of the flow turbulence

To receive the aerodynamic characteristics close to the real con-
ditions of structural member flowed by the turbulent lower atmo-
sphere layer, the air flow in the effective part of the wind tun-
nel was turbulizated by means of special nets with cells of dif-
ferent dimensions and different diameters of the wire. These nets
were set up in the wind tunnel nozzle section. The degree of the
flow turbulence is averaged after the measurements with the help
of the hot-wire anemometer longitudinally and transverse to the
flow in the model location area, at least in 10... 12 points. The
parameters of the turbulent nets are given in the Table 2   [2] .

Cell dimensions, mm	60 x 60	30 x 30	60 x 60	50 x 50	90 x 90
Wire diameter (bar), mm	0,5	0,5	6	10	20
Flow turbulence degree $\mathcal{E}$, %	0,8	1,5	2,5	6	8

Table 2   The parameters of turbulating nets

3.3 The experimental results

The results of the wind tunnel tests of models N 2 and N 3 are given in the Figures 1 and 2. These models turned out to be the most sensitive to the wind flow effect. It is confirmed by the character of the lift force change with the increase of the angle of attack. Three regions of angles of attack $0 < \alpha_1 < 15^\circ$; $85^\circ < \alpha_2 < 95^\circ$; $120^\circ < \alpha_3 < 160^\circ$ were discovered. In these regions the negative gradient $c_y^\alpha = dc_y/d\alpha$ surpasses by far the drag coefficient.

4. CONCLUSION

The analysis of the wind tunnel test results of all models made it possible to come to the following conclusions:

- there are three main regions of angles of attack, in which aeroelastic instability according to Den-Gartog self-excited galloping oscillations is possible to appear;

- the critical velocity of galloping is minimum for the model N 2 at the angles of attack in the region $\alpha_2 (c_y^\alpha + c_x = -7.6)$ and for the model N 3 at the angles of attack in the region α_1 $(c_y^\alpha + c_x = -1.4)$;

- the prediction of criteria of appearance and parameters of aeroelastic self-excited oscillations according to Den-Gartog at glaze-wind loads is possible to realize due to formulae [3]: for the critical velocity

$$V_{cr} = \frac{2 m \delta \omega_o}{-\left(c_y^\alpha + c_x\right) \pi \rho d} \quad ,$$

and for the amplitudes

$$\bar{a} = \frac{2V}{\omega_o d} \sqrt{1 - \frac{V_{cr}}{V}} \quad ; \quad \bar{a} = \frac{a}{d} \quad ; \quad V > V_{cr} ,$$

where δ, m, ω_o, d are, correspondingly, oscillation logarithmic decrement (at $V = 0$), linear mass, natural angular frequency of vibrations and midship section (at $\alpha = 0$).

REFERENCES

I. ЗАВАРИНА М.В. Строительная климатология. - Л., Гидрометеоиз-
дат, 1976. - 312 с.

2. ГРАФСКИЙ И.Ю., КАЗАКЕВИЧ М.И. Аэродинамика плохообтекаемых
тел: Учебное пособие. - Днепропетровск, ДГУ, 1983. - 116 с.

3. КАЗАКЕВИЧ М.И. Аэродинамическая устойчивость надземных и вися-
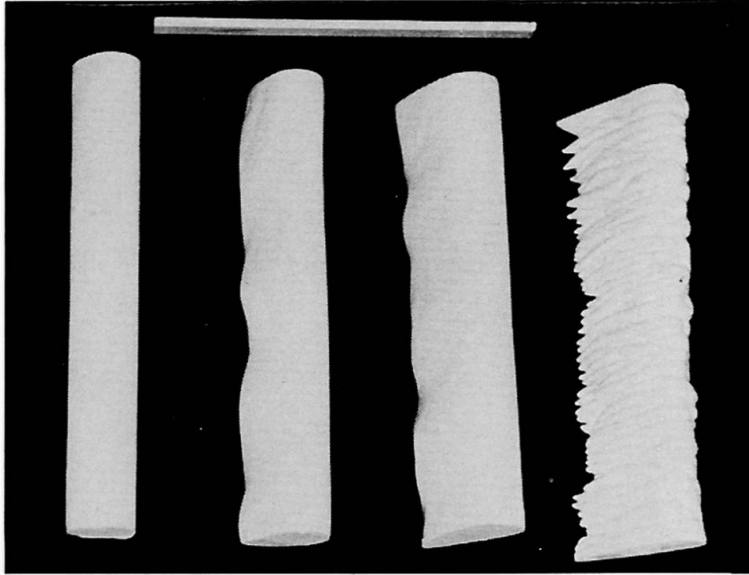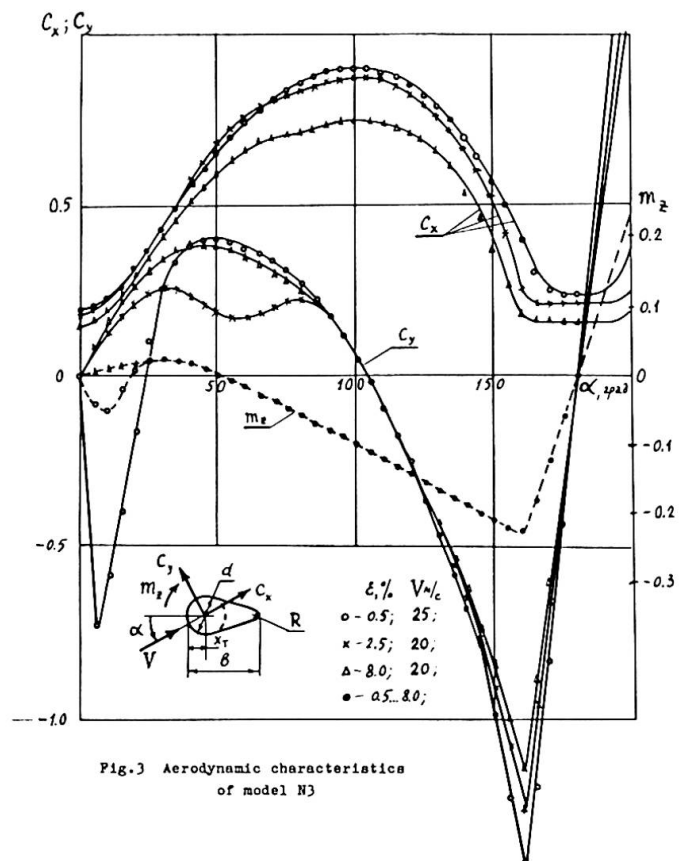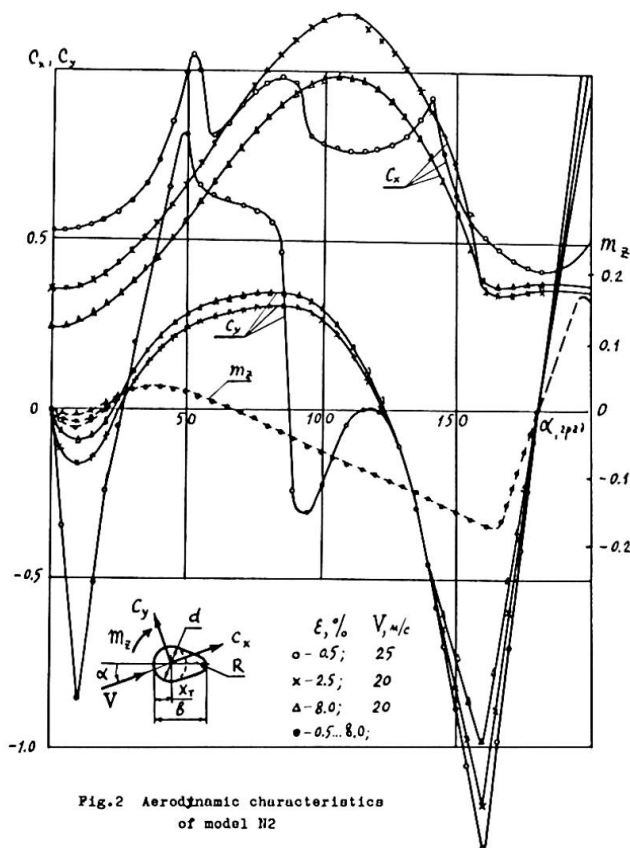чих трубопроводов. - М.: Недра, 1977. - 200 с.

Fig.1 The general view of models

Fig.2 Aerodynamic characteristics
of model N2

Fig.3 Aerodynamic characteristics
of model N3

Leere Seite

Blank page

Page vide

Snow Loads on Roofs

Charges de neige sur les toits

Schneelasten auf Dächer

Nick ISYUMOV
Assoc. Res. Dir.
Univ. of Western Ontario
London, ON, Canada

Mike MIKITIUK
Res. Assoc.
Univ. of Western Ontario
London, ON, Canada

Alan G. DAVENPORT
Prof., Dir.
Univ. of Western Ontario
London, ON, Canada

Nick Isyumov obtained his under-graduate degree in Engineering Science in 1960 and his Ph.D. in 1971, both from the University of Western Ontario. He is the Manager and Associate Research Director of the Boundary Layer Wind Tunnel Laboratory.

Mike Mikitiuk graduated in Civil Engineering from the University of Western Ontario in 1975. He received his M.E. Sc. in Civil Engineering also at the same institution in 1978. He is currently a Research Associate at the Boundary Layer Wind Tunnel Laboratory.

Alan Davenport, obtained his B.A. and M.A. from Cambridge University England in 1954 and 1958. In 1957 he received his M.A. Sc. from the University of Toronto and a Ph.D. from the University of Bristol in 1961. He is a Professor in Civil Engineering and the Director of the Boundary Layer Wind Tunnel Laboratory. He has advised on the Construction and design of a number of long span bridges and structures.

SUMMARY
This paper examines various properties of roof snow loads with emphasis on their variability and the reliability of snow load estimates used for design. A greater sensitivity to the action of climatic and meteorological variables and the influence of the roof aerodynamics tend to result in a variability higher than that found for ground snow loads. Situations, where the combined snow and wind loadings can become significant are identified and discussed.

RESUME
L'article présente quelques propriétés des charges de neige sur les toits, leur variation et la fiabilité des prédictions utilisées pour le projet. L'influence des conditions climatiques et météorologiques ainsi que l'influence de la forme aérodynamique du toit sont plus grandes que pour les charges de neige sur le sol. Des cas sont présentés où la combinaison de la charge de neige et de vent devient déterminante.

ZUSAMMENFASSUNG
Dieser Artikel stellt Betrachtungen an über verschiedene Eigenarten von Schneelasten auf Dächer, mit Betonung auf die Variabilität der Schneelasten und die Zuverlässigkeit von Abschätzungen für die Berechnung der Tragkonstruktion. Die Einflüsse auf die Variabilität der Schneelasten durch klimatische und meteorologische Parameter und durch die Aerodynamik des Daches sind grösser, als auf dem Erdboden festgestellt werden kann. Es werden Situationen genannt und erläutert, bei denen Kombinationen von Schnee- und Windlasten massgebend werden können.

1. INTRODUCTION

Accumulations of snow can impose significant loads on buildings and structures located in cold climates. The practical importance of these loads increases for longer span roof systems as used in stadiums, arenas, skating rinks, hangars etc. and generally for buildings and structures where the roof system represents a major portion of the construction cost. Snow loads, like other environmental loads, exhibit marked variability. Not only are there large regional variations due to climatic differences but within each region considerable variations occur from roof to roof and from winter to winter. While specified design snow loads have tended to be conservative, there is ample evidence in the literature (1,2) to demonstrate the dangers which can arise from an inadequate provision.

The complications which result due to large differences in the aerodynamic, thermal, and structural characteristics of roofs are compounded by the variability of climatic effects. Design snow loads contained in most building codes are based on annual extreme ground loads, expected to be exceeded with some acceptably small probability level. While suitable for conventional buildings and structures, loads arrived at from the cumulative effects of snowfalls over some period of time are not necessarily suited for structures designed not to accumulate snow. For example, snow melting systems are commonly used to maintain air-supported roofs or skylights clear of snow. For these types of structures there is on average no snow accumulation and the extreme loading tends to be dominated by effects resulting from single extreme storms. The diversity of possible structural systems, many with unusual requirements and sensitivities to snow imposed loads, also complicates the specification of design loads with clear implications on their overall reliability.

2. CURRENT PRACTICE

Roof snow loads currently specified in most building codes (1,2) are based on measurements of ground snow depth. In this approach L_r, the design snow load on the roof is expressed as,

$$L_r = C_s L_g \qquad (1)$$

where L_g is the snow load on the ground estimated for a selected return period and C_s is a snow load coefficient which relates the roof snow load to that on the ground. In Canada (1), L_g for a particular location is taken as the 30-year return period annual maximum ground snow depth converted to a load using a specific gravity of 0.192. The load corresponding to the maximum recorded 24-hour rainfall for the month during which the ground snow depth tends to reach a maximum is added to this value. Values of C_s contained in codes are based on empirical information and are selected to allow for reductions of the roof snow deposit due to the action of wind and slide-off and local increases in snow accumulation due to drift formation and in some cases the transfer of snow from higher to lower roofs by sliding. Some codes (2) also contains a factor which allows for heat losses from the building.

Although snow deposits on roofs and on the ground are influenced by the same meteorological and climatic processes, there are important differences in the details of the snow load formation (3,4,5). Generally, while the ground snow depth does represent a good measure of the snowfall and its persistence over the course of winter, it does not necessarily provide a reliable measure of snow loads formed on roofs. Despite these difficulties, the simplicity of the approach described by equation (1) is attractive, particularly since relationships between ground and roof snow loads have been improved and calibrated by extensive full-scale observation programs (6,7,8,9,10,11).

3. ALTERNATIVE METHODS

3.1 Overview

Physical scaled model tests in wind tunnels or water flumes can be used to provide information on snow deposition on roofs during particular snow storms (3,4). Unlike extreme winds effects which are caused by single events or storms, the formation of extreme snow loads, accept in relatively mild winter climates, tends to be formed by an accumulation of snow over a period of time. As a result, the magnitude of the maximum roof snow load depends on the time history of individual snowfalls and complex interaction of meteorological factors which can act to reduce, modify and, in some cases, increase snow deposits. In such situations the formation of extreme snow loads is clearly more difficult without a representative physical model. A mass balance approach has been developed to describe the snow accumulation process in terms of its basic meteorological and climatic parameters (3,4,12). In this approach, the roof snow load is taken as the running sum of incremental loads due to individual snowfalls and the depletion of the roof snow load by wind action and thermal ablation. Physical model tests are used to provide information on the deposition of snow during particular snowfalls and the depletion of the roof snow deposit by drifting. Wind is the dominate factor influencing both the magnitude and the distribution of snow deposits on roofs. During calm conditions the snow accumulation tends to be uniformly distributed with modifications due to slide-off from inclined surfaces. In the presence of wind the deposition of new snow on roofs tends to be non-uniform and snow depositions are further modified by drifting.

The influence of thermal effects are more difficult to address in physical model studies and must rely on mathematical and numerical modelling. Relatively simple approaches, using the air temperature as an index, are possible to estimate the ablation of snow due to melting and the inhibiting effects of surface melting and refreezing on the drifting action of wind.

3.2 Numerical Simulation of Snow Load Formation

A Monte Carlo computer simulation technique has been developed (3,4,12) to simulate, on a day-by-day basis, the history of the snow load on particular roofs. Repeating this simulation over a large number of winters, provides statistical information on snow load extremes required in design. Suitable statistical models of such climatic variables as the depth and water equivalent of the daily snowfall, the wind speed and wind direction, and the atmospheric temperature used in the simulation are given elsewhere (3,4,12).

A Weibull distribution has been found to provide a good statistical model of daily snowfall depths S. Here the probability of exceeding a particular value of S during a particular month denoted by t and in the general form including the dependence of the daily snowfall on the direction of the wind during a snow storm is of the form,

$$P\,(>S,t,\theta) = m\,(t,\theta)\,exp - \{S/C\,(t,\theta)\}^{K\,(t,\theta)} \qquad (2)$$

Here $P\,(>S,t,\theta)$ is the probability of exceeding a daily snowfall depth of S during month t and during wind conditions with a wind direction θ, and $m\,(t,\theta)$ is the expectation of snowfall during month t and $C(t,\theta)$ and $K(t,\theta)$ are Weibull parameters for the same month and wind direction. The parameter K generally is less than 1.0 and does not vary significantly over the course of the winter. The parameter C is a measure of the magnitude of the snowfall. The expectation m provides a measure of the length of the snowfall season and tends to peak near mid-winter. All three parameters tend to vary regionally. Either continuous or sector-by-sector variations of the parameters can be used. Typical probability distributions of the daily snowfall during snow storms associated with different wind directions are indicated in Figure 1. The distribution for Ottawa includes the entire winter, that for Chicago is for the

month of January. The probability of exceeding a particular snowfall amount varies markedly with wind direction. This is not unexpected as the local snowfall tends to be highly sensitive to the local geography. The pronounced easterly lobe for Chicago reflects the influence of Lake Michigan.

The water equivalent of new snow used in the Monte Carlo simulation so far has been based on the analysis of daily precipitation data. A summary of the mean water equivalent of new snow and its dependence on the average daily air temperature is given in Figure 2. The average water equivalent is approximately around .1 with coefficients of variation, depending on location, ranging in the order of 20 to 50%.

3.3   Relationship Between Roof and Ground Loads

Snow loads on roofs on average tend to be significantly lower than those on the ground. Nevertheless, in certain circumstances larger than ground snow loads can be experienced on roofs. Figure 3 provides a summary of the daily roof snow load expressed as a ratio of the corresponding ground load. These results are from a Monte Carlo simulation for exposed flat roofs. The average value of L_r/L_g or the roof snow load coefficient C_s, on a daily basis, is seen to be of the order of 0.3 and less. The variability of L_r/L_g for one of the stations is shown for ground snow loads which corresponds to about .5 and .9 of the 30-year extreme value. The distributions are highly skewed and C_s, on a day-to-day basis, occasionally exceeds 1.0 (see the histogram given for $L_g/L_g (30) = 0.5$). This is consistent with available field observations which suggests that the roof snow load can in certain circumstances exceed that on the ground.
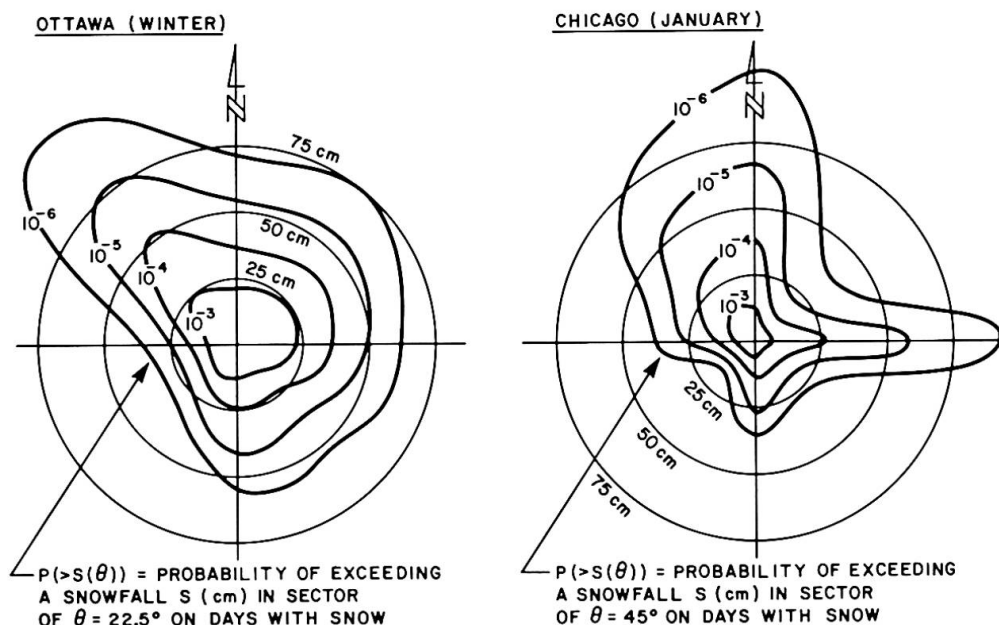
OTTAWA (WINTER)   CHICAGO (JANUARY)

P(>S(θ)) = PROBABILITY OF EXCEEDING
A SNOWFALL S (cm) IN SECTOR
OF θ = 22.5° ON DAYS WITH SNOW

P(>S(θ)) = PROBABILITY OF EXCEEDING
A SNOWFALL S (cm) IN SECTOR
OF θ = 45° ON DAYS WITH SNOW

Fig. 1   **Probability Distribution of Daily Snowfall During Wind Conditions Associated With Differnt Wind Directions**

General trends observed for annual maxima, obtained from a Monte Carlo simulation for exposed flat roofs, are as follows:

i)   Annual maximum roof and ground snow loads rarely occur on the same day.
ii)   Maximum roof load tends to be well below those on the ground.
iii)   The correlation between the annual maximum roof and ground snow loads tends to be small. Typical correlation coefficients using a linear relationship tend to be generally less than .5 which is consistent with full-scale observations.
iv)   The relationship between the extreme roof and ground snow loads is influenced by the statistical properties of local snowfall, air temperature, wind speed and wind

direction climates. Extreme roof snow loads tend to be least in comparison with those on the ground for locations with well-below-freezing temperatures and where the ground snow load represents the accumulation of a large number of relatively small snowfalls. The ratio of roof-to-ground snow loads on the other hand tends to be largest for relatively warm winter climates where a few events dominate the entire winter snowfall.
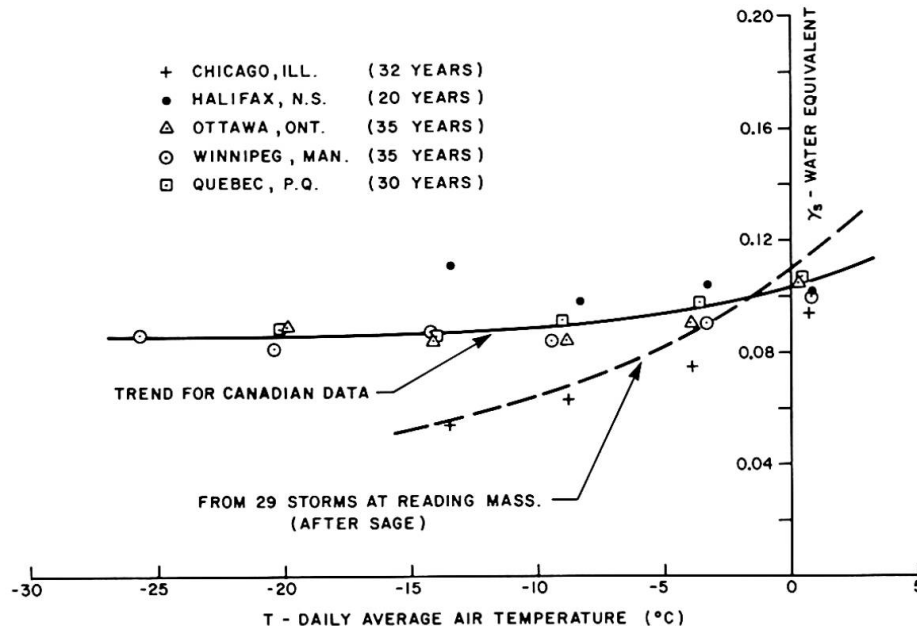

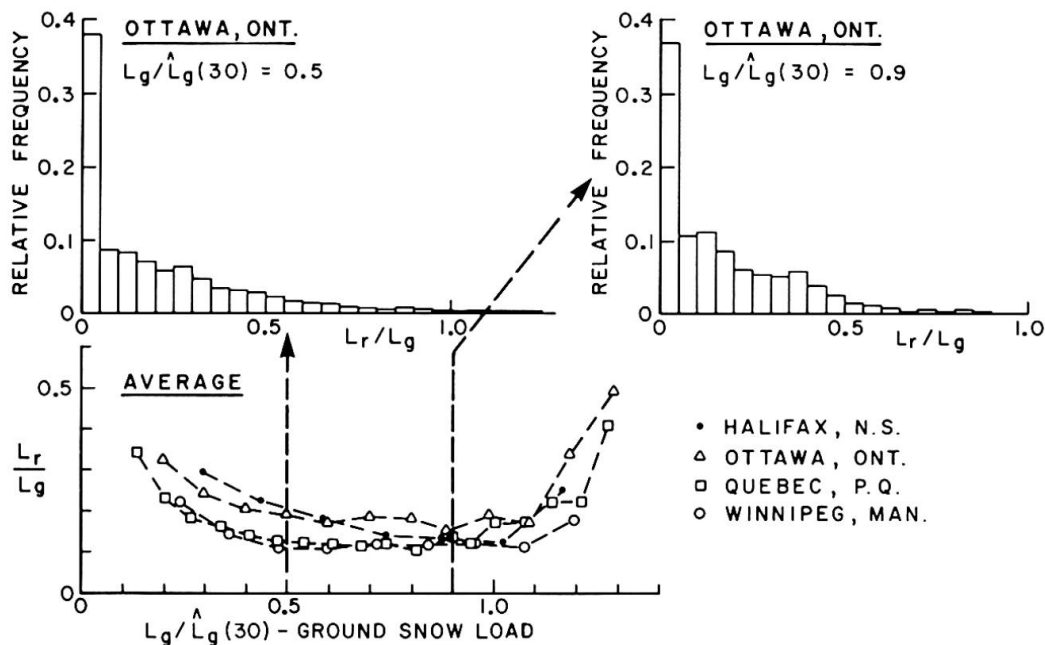**Fig. 2**   **Mean Water Equivalent of New Snow and Its Dependence on Temperature**

Fig. 3   **Ratio of Daily Roof Snow Load to the Ground Loads; From Monte Carlo Simulation for Exposed Flat Roofs**

4. VARIABILITY

The variability of roof snow loads is consistently greater than that of the ground snow load. This is illustrated by the results of Monte Carlo simulations of extreme

loads on the ground and on flat roofs, seen in Fig. 4. A Type I extreme value distribution is used to fit the extremes. To improve the comparison, the annual extremes have been normalized by their respective modal value. The coefficients of variation of the annual maximum ground and roof snow loads are respectively about 0.26 and 0.57. Coefficients of variation of the annual and lifetime extreme ground and roof snow loads are shown in Table 1 for 4 locations. The individual annual extremes in this analysis are taken to be independent and the lifetime M is taken as 30 years. Large differences in the coefficients of variation are seen particularly for the annual extremes.

Treating the roof snow load coefficient C_s in equation 1 as an independent random variable, provides an estimate of its coefficient of variation in terms of V_{L_r} and V_{L_g} (see equation 3). A load factor, defined as the ratio of the design roof snow loads to its 30-year expected value can be expressed as shown in equation 4. Values of the coefficient of variation of C_s and the load factor γ are given in Table 2 for exposed flat roofs based on a lifetime of 30 years. The values of C_s are in the order of 15 percent and the load factors are comparable to the value of 1.5 specified for limit states design in the Canadian National Building Code (1). A greater variability and hence larger values of γ are expected for more complex roof shapes.

$$V_{C_S} \simeq (V_{L_r}{}^2 - V_{L_g}{}^2)^{\frac{1}{2}} \tag{3}$$

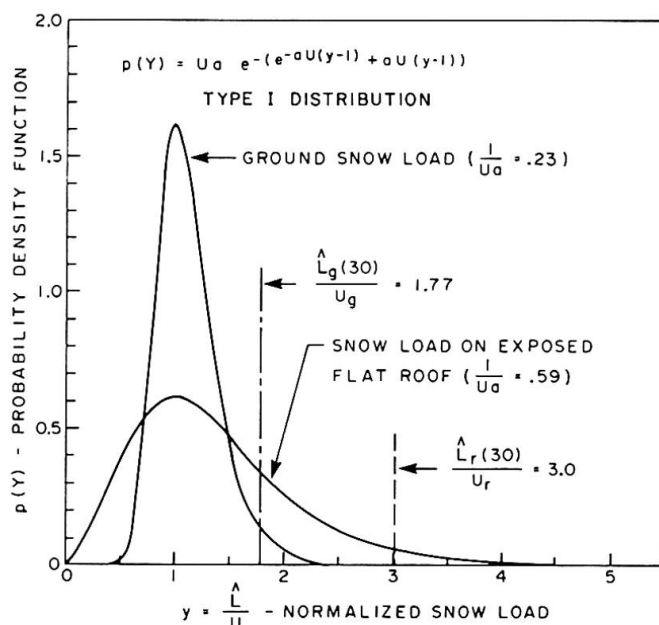$$\gamma = \frac{L_{r_{design}}}{L_{r_{expected}}} = \exp(1.65\,V_{L_r}) \tag{4}$$

Fig. 5　　**Typical Extreme Value Distributions of Ground and Roof Snow Loads; From Monte Carlo Simulation for Exposed Flat Roofs**

4.1　Duration of Snow Loads

The simulated time histories of snow loads allow an analysis of the duration associated with particular load magnitudes. In this case the duration is taken as the uninterrupted dwell time associated with a particular exceedance of a load level. As a first approximation, the duration of a particular snow load level can be taken to follow an exponential distribution as given in equation 5. Here a is a parameter of the

distribution equal to its mean value and its standard deviation. Estimates of the duration of ground and roof snow loads corresponding to their respective 30-year return period values were estimated for exposed flat roofs at several locations. As one would anticipate, the durations of roof snow loads tend to be well below those of the ground loads. For the Halifax, Ottawa, Quebec City and Winnipeg areas, the average durations of the 30-year return period ground snow loads are found to be 18, 14, 13 and 33 days, respectively. The corresponding durations of the 30-year roof snow load, however, were found to be about 9, 10, 10 and 19 days respectively. A shorter exposure to the design load is seen to be a distinct advantage.

$$P \ (> T) = e^{-aT} \tag{5}$$

4.2   Joint Action of Snow and Wind Loads

Available climatic information indicates that occurrences of extreme wind and snow loads can be treated as statistically independent events. As a result, it is reasonable to use a joint action or load combination factor in situations of combined loading. This allows for the reduced likelihood of a simultaneous occurrence of an extreme wind and snow load. A value of 0.75 for this factor as used by NBC (1), is not inappropriate.

Generally wind and snow loads on roofs tend to act in opposite directions and some aerodynamic insight is required to identify situations where these loads can be additive. Some schematic representations of combined snow and wind loads are shown in Fig. 5. While cases ii) and iii) would normally be recognized, the possibility of experiencing positive or downward acting wind pressures on low roofs adjacent to a taller building tends to be overlooked. This can be an important load case as large snow drift deposits can accumulate near changes in elevation. Finally, the combined action of snow and wind tends to accentuate load non-uniformities and can be important for structures sensitive to unbalanced loadings.
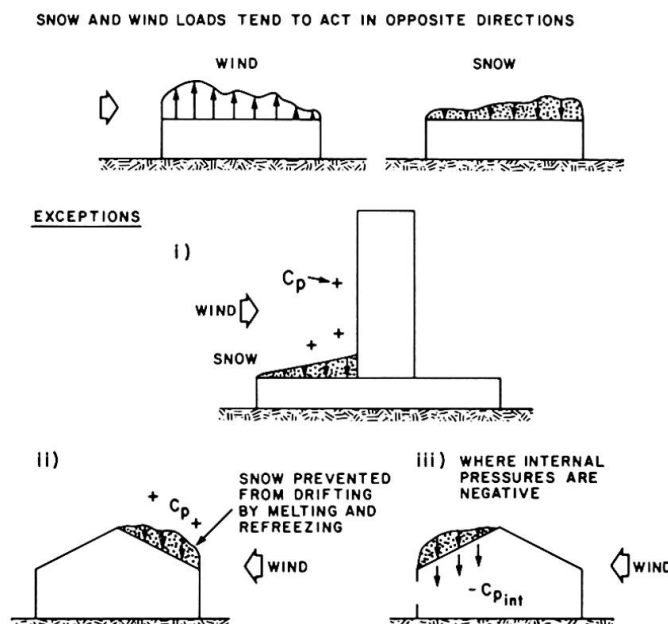

Fig. 5   Combined Snow and Wind Loads on Roofs

5.   CONCLUSIONS

The emergence of new types of structural forms for longer-span roof systems necessitates a review of existing snow load design procedures which may not be fully

suited for these new systems. An alternative design approach, using a Monte Carlo simulation of the winter climate, has been used to examine the characteristics of snow loads on flat roofs located in cold and moderately cold winter climates. Statistical descriptions of the various meteorological variables, required in the computer simulation are generally available. This, combined with a growing body of full-scale data is expected to lead to improvements in the reliability of design snow loads.

TABLE 1
Coefficients of Variation of Simulated Annual and Lifetime Extreme Snow Loads on Exposed Flat Roofs at Several Locations

Station	Annual Extremes		Lifetime Extremes (M = 30)	
	V_{L_r}	V_{L_g}	$(V_{L_r})_M$	$(V_{L_g})_M$
Halifax, N.S.	0.65	0.55	0.24	0.21
Ottawa, Ont.	0.54	0.34	0.22	0.18
Quebec City, P.O.	0.51	0.30	0.21	0.16
Winnipeg, Man.	0.58	0.31	0.23	0.17

TABLE 2
Coefficients of Variation of C_S and Load Factors for Lifetime Extreme Roof Snow Loads; Exposed Flat Roofs (M = 30 Years)

Station	V_{C_S}	Load Factor γ
Halifax, N.S.	.12	1.49
Ottawa, Ont.	.13	1.44
Quebec City, P.Q.	.14	1.41
Winnipeg, Man.	.15	1.46

6.   REFERENCES

1.   National Building Code of Canada (NBC)., N.R.C.C. Publ. No. 17303, 1980.
2.   American National Standard for Minimum Design Loads for Buildings and Other Structures, ANSI A58.1 - 1982, 1982.
3.   Isyumov, N., "An Approach to the Prediction of Snow Loads", Ph.D. Thesis, University of Western Ontario, Eng. Sci. Res. Rep. BLWT-9-71, 1971.
4.   Isyumov, N. and Davenport, A. G., "A Probabilitic Approach to the Prediction of Snow Loads", Can. J. Civil Eng. I(1): 28-49, 1974.
5.   Isyumov, N., "Roof Snow Loads: Their Variability and Dependence on Climatic Conditions", Symp. Uses of Wood in Adverse Environments, Van Nostrand 1982.
6.   Lutes, D. A. and Schriever, W. R., "Snow Accumulations in Canada: Case Histories: II"", N.R.C.C., Div. Build. Res. Tech. Paper No. 339, 1971.
7.   Schreiver, W. R. and Otstavnow, V. A., "Snow Loads: Preparation of Standards for Snow Loads on Roofs in Various Countries With Particular Reference to the U.S.S.R. and Canada", C.I.B., Res. Rep. No. 9, 1967.
8.   Taylor, D. A., "Snow Loads for the Design of Cylindrical Curved Roofs in Canada", Can. J. Civil Eng., 8(1), 63-76, 1981.
9.   Tobiasson, W. and Redfield, R., "Alaskan Snow Loads", 24th Alaskan Science Conf., Univ. of Alaska, 1973.
10.   O'Rourke, M., Koch, P. and Redfield, R., "Analysis of Roof Snow Load Case Studies", CRREL Report 83-1, 1983.
11.   O'Rourke, M. J., Speek, R. and Urick Stiefel, "Drift Snow Loads on Multi-Level Roofs", Dept. Civil Eng. Rep., Rensselaer Polytechnic Inst., Troy, N.Y., 1984.
12.   Isyumov, N. and Mikitiuk, M., "Climatology of Snowfall and Related Meteorological Variables With Application to Roof Snow Load Specifications", Can. J. Civil Eng. 4(2): 240-256, 1977.
13.   Sage, J. D., "An Operational Model for Hourly Snowfall", Proc. of the 33rd Annual Eastern Snow Conference, Glens Falls, N.Y., U.S.A., 1976.

Conclusions to Seminar VIII
Snow and Ice Effects on Structures

R.L. BOOTH
Chairman
Carruthers & Wallace Ltd
Toronto, ON, Canada

Professor Allan Davenport presented the first paper, entitled "Snow and Wind Loads on Roofs" and which was co-authored by N. Isyumov and M. Mikitiuk, also of the University of Western Ontario, Boundary Layer Wind Tunnel.

The presentation introduced the need to reconcile the physical characteristics of snow with the meteorological characteristics of the site. Particular attention was drawn to the choice of appropriate "conversion factors" for use in establishing roof snow loadings based on measured, ground snow accumulations.

The speaker referred to the information provided by the National Building Code of Canada and the Division of Building Research of the National Research Council of Canada for determining the allowances for unbalanced snow loading caused by wind action. Also described, were the current laboratory techniques for the determination of qualitative and quantitative values for the variation in snow deposition on roofs. The uses of water flumes and wind tunnels for this purpose were noted.

The paper went on to suggest the choice of load combination factors for specific roof geometries, based on observed maximum combined wind and snow loads compared with maximum wind and snow loads acting independently. The proposed laboratory simulation for forecasting snow loads for specific roof structures in specific locations was described by the speaker as relatively crude at present but promising for the future.

The second paper "Damages due to Snow Loads", was presented by Dr. Bengt Johannesson.

The paper describes a comprehensive study of the structural damage and failures which occurred in Sweden during the relatively severe winter of 1976-77. Most of the structures were of timber or light weight steel construction.

The failures of a number of example structures were described in detail. The authors pointed out that a significant number of the failures were caused by "manufacturing faults", (fabrication/construction did not conform to design) and "underdesign" (mistakes or other deficiencies in the design calculations). "Excessive snow load" the third cause, resulted usually from improper consideration of snow drifting.

Of interest was the authors' reference to the difficulties experienced in obtaining reliable information concerning structural failures. For this reason, it was emphasized that caution must be used in accepting as fact, information not supported by proven evidence.

The speaker concluded with the observation that, in general, structures with high snow load to dead load ratios were most susceptible to failure. Such structures, typically of timber and light weight steel, require special care in their design and construction.

Professor Edo Hemerich presented the third paper entitled "Determination of Design Snow Loads".

This paper proved to be a logical follow-up to the second paper in that it recognized the tendency for light weight structures to have a lower degree of safety under snow loading. A means of establishing a formula which provides for a uniform degree of safety was described. The method is based on statistical data on snow fall for specific locations, dead load to snow load ratios, and data obtained from the analyses of the reliability index of existing structures. Also in the formula, the probabilistic characteristics of resistance must be determined from statistical data on the actual material being used.

The formula for calculating snow load, after values for all the required parameters are inserted, indicates the design snow load for a flat roof at a constant degree of safety.

The final paper was presented by Josef Grob, civil engineer of Basle Switzerland. His presentation described the extremely innovative design and construction of a cable suspended pipeline over a glacier in the Swiss Alps.

The suspension cables for the pipeline extend more than 857 m from a fixed low anchorage tripod at elevation 2700 m to the high anchor at 2981 m. Of particular interest is the intermediate support for the cables which is founded on the glacier itself at approximately elevation 2780 m. This support consists of a 35 m pylon, restrained by 4 guy cables which are anchored in the glacier. The design allows for the surface, downhill creep of the glacier (15-20 m per year). A total displacement of 50 m parallel to the suspension cables and 10 m transverse can be accommodated, after which the pylon may be removed and re-erected as necessary.

The presentation of these four papers made for a very interesting and informative seminar, as evidenced by the response of the audience during the question periods.